



Molecular layer deposition (MLD) modified SSZ-13 membrane for greatly enhanced H₂ separation

Qiaobei Dong^a, Ji Jiang^a, Shiguang Li^b, Miao Yu^{a,*}

^a Department of Chemical and Biological Engineering, Rensselaer Polytechnic Institute, Troy, NY, 12180, United States

^b Gas Technology Institute, Des Plaines, IL, 60018, United States

ARTICLE INFO

Keywords:

Molecular layer deposition
SSZ-13 membrane
H₂ separation

ABSTRACT

Zeolite membranes with high thermal stability and well-fined pores are attractive for gas separation. However, the defects are almost inevitable in zeolite membranes. Moreover, fine-tuning zeolitic pores for precise molecular separation is challenging. In this study, molecular layer deposition (MLD) was employed to deposit ultrathin microporous coating on SSZ-13 zeolite membrane. **The MLD modified SSZ-13 composite membrane was highly selective for H₂ separation. With optimized MLD cycles, H₂/N₂ and H₂/CH₄ ideal selectivities as high as 35.6 and 427, respectively, were obtained, in strong contrast with approximately 5 for base SSZ-13 membrane.** These results suggest that MLD is a very promising technology to precisely modify the pore size of zeolite membranes, while minimizing flow through non-selective defects, for gas separation.

1. Introduction

Hydrogen, as a clean fuel, has attracted numerous attentions and shown great potential for alleviating the growing energy crises [1]. Tremendous technologies have been conducted to explore the H₂ separation and purification, such as cryogenic distillation, adsorptive separation, and membrane technology [2,3]. Among these technologies, membrane separation with features of low energy consumption, easy to operate, and lower capital cost, indicates itself as an excellent candidate [4–6].

Inorganic membranes, especially zeolite membranes with well-defined crystalline pores, were broadly investigated for H₂ separation [7–9]. Nevertheless, the grain boundary defects are almost inevitable during the hydrothermal synthesis and high-temperature thermal treatment for removing the structure-directing agents, which significantly deteriorate the separation performance of zeolite membranes [10]. To improve the membrane quality, growth of thicker membranes and/or post-treatment by modification of zeolitic/non-zeolitic pores are feasible. In recent years, various post-treatment methods were developed for modification of zeolite membranes [11–14]. For instance, Hong et al. [15], applied a catalytic cracking deposition method to modify ZSM-5 membranes, as methyldiethoxysilane with a smaller molecular size than the pore size of ZSM-5 (0.55 nm) was adsorbed and cracked into the zeolitic pores to reduce the effective pore size. To eliminate the

non-zeolitic defects on zeolite membrane surface, chemical vapor deposition was employed to deposit tetraethyl orthosilicate or tetramethoxyl silane on zeolite membranes, because these molecules are too large to enter the pores of various zeolites [16]. However, these techniques are usually complicated and employ high-temperature treatments, which might also lead to the formation of cracks and/or grain boundary defects during the modification process [10]. Therefore, simpler methods are necessary for the modification of zeolite membranes on a large scale.

Molecular layer deposition (MLD), which utilizes self-limiting surface reactions to generate hybrid organic-inorganic thin coatings on various substrates, has been demonstrated to be an effective way for precise control of pore sizes of porous materials [17–19]. Furthermore, the dense hybrid thin coatings can be converted into porous layers by removing the organic compound via facile thermal treatment. Recently, we demonstrated a “pore misalignment” concept by forming ultrathin microporous coatings on the external surface of zeolites for fine-tuning their pore mouth size so smaller gas molecules can penetrate into zeolite pores while the large ones will be blocked [20,21].

In this study, **SSZ-13 (crystalline pore size: 0.38 nm) membrane was modified by MLD in an attempt to narrow the crystal pore mouth to the size close to H₂ (kinetic diameter: 0.289 nm) while reducing flow through non-selective defects/inter-crystalline pores, as shown schematically in Fig. 1.** Single gas permeances were measured and compared

* Corresponding author.

E-mail address: yum5@rpi.edu (M. Yu).

<https://doi.org/10.1016/j.memsci.2020.119040>

Received 30 October 2020; Received in revised form 22 December 2020; Accepted 30 December 2020

Available online 6 January 2021

0376-7388/© 2021 Elsevier B.V. All rights reserved.

for SSZ-13 membrane before and after MLD modification. Binary mixture separation properties of H_2/N_2 and H_2/CH_4 were also evaluated for both pristine and modified membranes. Compared with the pristine SSZ-13 zeolite membrane, the H_2/N_2 and H_2/CH_4 selectivities were significantly increased after optimized MLD cycles.

2. Experimental

2.1. Chemicals

Colloidal silica (Ludox SM-40), aluminum hydroxide ($Al(OH)_3$), sodium hydroxide (NaOH, 98%), titanium tetrachloride ($TiCl_4$, >99.995%) and ethylene glycol (EG, 99.8%) were purchased from Sigma-Aldrich. N,N,N-trimethyl-1-adamant ammonium hydroxide (TMAdaOH, 25.7%) was purchased from MuseChem, Inc. H_2 (99.999%), N_2 (99.999%), CO_2 (99.999%), O_2 (99.999%), CH_4 (99.99%) were purchased from Airgas, Inc.

2.2. Preparation of SSZ-13 zeolite membrane

SSZ-13 zeolite crystals were prepared according to a procedure described by Zones et al. [22]. The molar composition of the gel was: $100 SiO_2:2.5 Al_2O_3:10 Na_2O:40 TMAdaOH:4400H_2O$. The gel was prepared by mixing TMAdaOH, NaOH, and $Al(OH)_3$ into DI water until $Al(OH)_3$ was fully dissolved. Then colloidal silica was dropwise added into the solution under magnetic stirring. The synthesis gel was stirred for 3 h before it was transferred to a Teflon-lined autoclave for synthesis. After synthesized at 433 K for 96 h, the obtained SSZ-13 zeolite crystals were thoroughly washed with DI water and dried at 373 K overnight. Finally, SSZ-13 zeolite crystals were calcined at 823 K for 10 h with heating and cooling rates of 5 K/min to remove the template. SSZ-13 zeolite membranes were hydrothermally synthesized on the external surface of Al_2O_3 hollow fibers by the secondary growth method. The precursor composition used for SSZ-13 membrane synthesis was the same as that of seed gel. Before membrane synthesis, the supports were coated with 2 wt% seed suspension for 10 s using a dip-coating method.

Then the membranes were hydrothermally synthesized at 433 K for 96 h in Teflon-lined autoclaves in the oven. After synthesis, the membranes were thoroughly washed and immersed in DI water overnight and finally calcined at 823 K for 10 h with heating and cooling rates of 1 K/min.

2.3. Modification of SSZ-13 membrane by MLD

$TiCl_4$ and EG were served as precursors of MLD to deposit titanium alkoxide on SSZ-13 and MFI membranes at 373 K in a tubular reactor. Both ends of the SSZ-13 membrane were wrapped with Teflon tape to prevent the deposition of titanium alkoxide on the inside of the membrane. Before MLD, SSZ-13 membrane was degassed at 493 K for 6 h to remove the adsorbed water. Then, $TiCl_4$ and EG were separately dosed into the reactor by the driving force of their room temperature vapor pressures. Ultrahigh purity N_2 was served as the purge gas to remove the excess precursors and byproducts during the reaction. A typical cycle includes the following sequence: $TiCl_4$ dose (60 s), N_2 purge and evacuation (300 s), EG dose (120 s), N_2 purge and evacuation (300 s). This process was program controlled by a LabVIEW software (2012, National Instruments). The detailed deposition process was described in our previous studies [20,21]. After MLD, a calcination process at 523 K for 2 h in air with both heating and cooling rate of 1 K/min was conducted to remove the organic compound of the deposited layer, thus converting the dense coating layer to porous layer.

2.4. Characterization

Field emission scanning electron microscopy (FE-SEM, Zeiss SUPRA 55) was used to characterize the surface morphology and thickness of SSZ-13 membrane. The crystal structure of pristine and modified SSZ-13 membranes were characterized by X-ray diffraction (XRD, Bruker D8-Discover instrument). The thickness of the MLD coating was measured by a focused ion beam SEM (FIB-SEM, FEI Versa 3D Dual Beam).

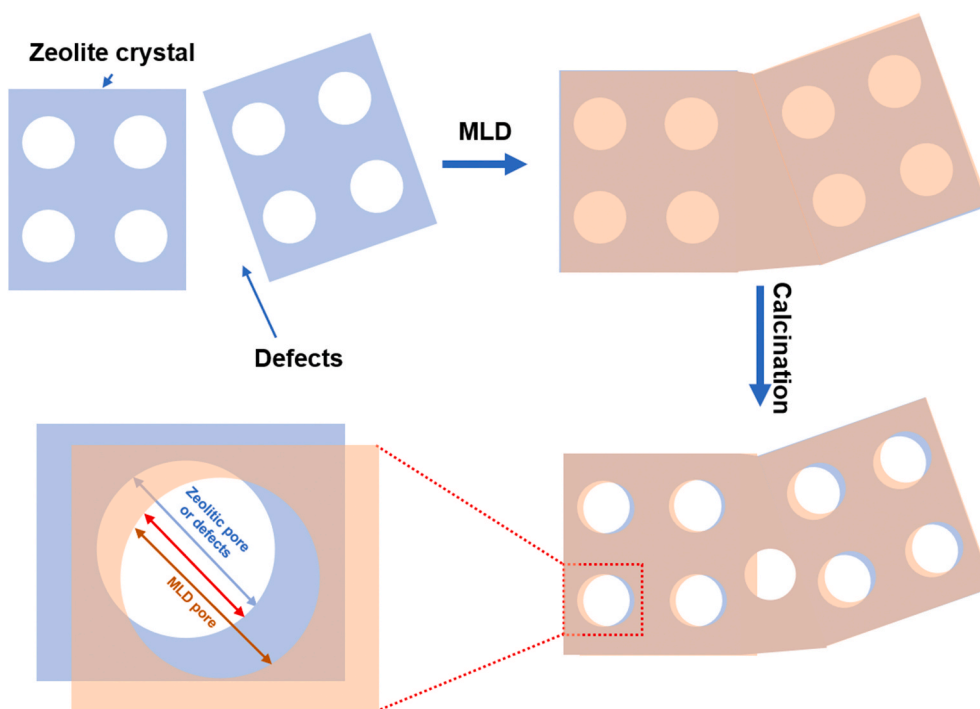


Fig. 1. Schematics illustration of surface crystal pore mouth reduction by pore misalignment and defects flow restriction via MLD on polycrystalline zeolite membrane.

2.5. Gas permeation

Single gas permeation and H_2/N_2 , H_2/CH_4 mixture gas separation experiments were conducted on SSZ-13 membrane before and after MLD to investigate the effect of the MLD on gas permeation. For the gas permeation test, the membrane was mounted in a dead-end mode in stainless steel module (Fig. S1). The membrane was sealed into the membrane module using the high-temperature epoxy. Before the gas permeation test, the membrane was in-situ degassed at 473 K for 2 h to remove the water adsorbed on the membrane. The feed pressure was modulated by a pressure regulator and monitored by an electronic transducer. The permeate side was operated under atmosphere pressure, and the permeation rate was measured by a soap film flowmeter.

Binary H_2/N_2 (50%/50%) or H_2/CH_4 (50%/50%) mixture separation was conducted at a feed pressure of 2 bar. No sweep gas was used in all gas permeation test. The retentate and permeate compositions were analyzed by a gas chromatograph (Agilent 6890), and the flow rates were measured by a soap film flowmeter. The gas permeance was calculated as the flux divided by the partial pressure driving forces, and separation selectivity is the ratio of permeances. Detailed calculated processes were published in our previous study [23].

3. Results and discussion

The surface and cross-sectional scanning electron microscopy (SEM) images of SSZ-13 membrane were shown in Fig. S2. A dense membrane layer with well-intergrown zeolite crystals can be observed, similar to those reported in the literature [24]. The cross-sectional SEM image revealed that the thickness of the SSZ-13 membrane was 8 μm . No obvious large defects, such as cracks or pinholes, were observed. X-ray diffraction (XRD) patterns shown in Fig. S3 indicated a pure phase of SSZ-13 with high crystallinity. No obvious change in the crystal structure and microstructure morphology were found after MLD treatment (Fig. S3 and Fig. S4). These results suggested that the formed hybrid coating by MLD should be an ultra-thin amorphous layer. Since the formed hybrid MLD coating is expected to be dense and impermeable as indicated by our previous work [20,21,25], H_2 permeance lower than $10^{-12} \text{ mol m}^{-2} \text{ s}^{-1} \cdot \text{Pa}^{-1}$ (measured at 10 bar) also suggested the full coverage of zeolite membrane surface after ≥ 20 cycles of MLD. This dense hybrid coating was subject to calcination in air at 523 K to

generate a porous layer, following our previous procedure [25].

Focused ion beam scanning electron microscopy (FIB-SEM) image (Fig. 2) showed that the average thickness of the ultrathin porous coating layer generated by 30 cycles of MLD and subsequent calcination was approximately 20 nm. Single-gas permeation for H_2 , CO_2 , O_2 , N_2 , and CH_4 through pristine and MLD modified SSZ-13 membranes was carried out at 473 K and 10 bar transmembrane pressure drop with permeate pressure of 1 bar, and the results were shown in Fig. 3a. For pristine SSZ-13 membrane, gas permeance generally decreased with the increase of the kinetic diameter, suggesting increased gas permeation resistance as their sizes approaching the crystal pore size of the SSZ-13. CH_4 permeance was similar to that of smaller O_2 and N_2 molecules, although its size is very close to the crystal pore size of SSZ-13. This may suggest the existence of defects in pristine SSZ-13 membrane. The H_2/CO_2 , H_2/N_2 , and H_2/CH_4 ideal selectivities of 1.4, 5.1 and 5.2, respectively, were calculated for the pristine SSZ-13 membrane. After MLD treatment, gas permeance decreased as compared with the pristine SSZ-13 membrane, suggesting that the membrane structure is denser and effective pore size becomes smaller. However, the MLD modified SSZ-13 membranes had a more pronounced effect on gases with larger size (N_2 and CH_4), leading to the significant increase of the H_2/N_2 and H_2/CH_4 ideal selectivities from 5.1 to 5.2 for pristine SSZ-13 membrane to 35.6 and 427 for SSZ-13 membrane after 30 cycles of MLD and calcination (SSZ-13+30MLD; similar abbreviation in the following context). These H_2/N_2 and H_2/CH_4 ideal selectivities are much higher than those of Knudsen selectivities (3.74 for H_2/N_2 and 2.83 for H_2/CH_4) [26], suggesting that gas transport through the MLD modified SSZ-13 membrane should be dominated by molecular sieving effect and effective pore size is probably very close to N_2 but smaller than CH_4 . SSZ-13+30MLD and SSZ-13+40MLD membranes showed similar CH_4 permeance ($1.0 \times 10^{-10} \text{ mol m}^{-2} \text{ s}^{-1} \cdot \text{Pa}^{-1}$) and N_2 permeance ($\sim 1.0 \times 10^{-9} \text{ mol m}^{-2} \text{ s}^{-1} \cdot \text{Pa}^{-1}$). Since CH_4 is close to the SSZ-13 crystal pore size, very low CH_4 permeance through SSZ-13 membrane with 30 or more MLD cycles suggested almost all non-zeolitic pores be covered by MLD coating. In addition, significantly decreased N_2 permeance indicated the SSZ-13 crystals pores on the membrane surface must have been reduced by MLD via pore misalignment, as suggested by our previous studies [20, 21,25].

Fig. 3b shows H_2 permeance gradually decreased with MLD cycles, which could be attributed to the increase of the mass transfer resistance in the membrane layer. Nevertheless, both H_2/N_2 and H_2/CH_4 ideal selectivities first increased and then slightly decreased with the increase of MLD cycles and reached a maximum at 30 cycles of MLD. This can be attributed to the relative reduction of gas permeation through surface zeolite pores and non-zeolitic pores. With less than 30 MLD cycles, MLD coating may gradually block non-zeolitic pores, leading to improved membrane quality and thus higher selectivity. With more than or equal to 30 cycles, transport resistance through zeolite pores might be suppressed more than that through non-zeolitic pores, and thus selectivity started to decrease. At the optimum MLD cycles of 30, a H_2 permeance of $4.27 \times 10^{-8} \text{ mol m}^{-2} \text{ s}^{-1} \cdot \text{Pa}^{-1}$ with H_2/N_2 and H_2/CH_4 ideal selectivities of 35.6 and 427, respectively, were obtained on SSZ-13+30MLD. We made a comparison between our membranes and other reported zeolite membranes in Table S1. Our H_2 permeance is comparable or slightly lower than that of reported zeolite membranes, but H_2/CH_4 selectivity is approximately 10 times higher because of the reduced pore size.

Fig. 4 showed equimolar H_2/N_2 and H_2/CH_4 mixture gas separation by SSZ-13+30MLD in a temperature range of 373–473 K and a pressure drop of 2 bar. Both H_2 permeance and H_2/N_2 or H_2/CH_4 selectivity increased with temperature. Nevertheless, H_2 permeance in H_2/CH_4 mixture was lower than that in H_2/N_2 mixture at all the testing temperatures, which could be attributed to the blockage of the narrowed surface zeolite pore mouth and SSZ-13 zeolite pores by the large CH_4 molecules. Increase of the H_2 permeance with the increasing temperature for the SSZ-13+30MLD membrane could be explained by the

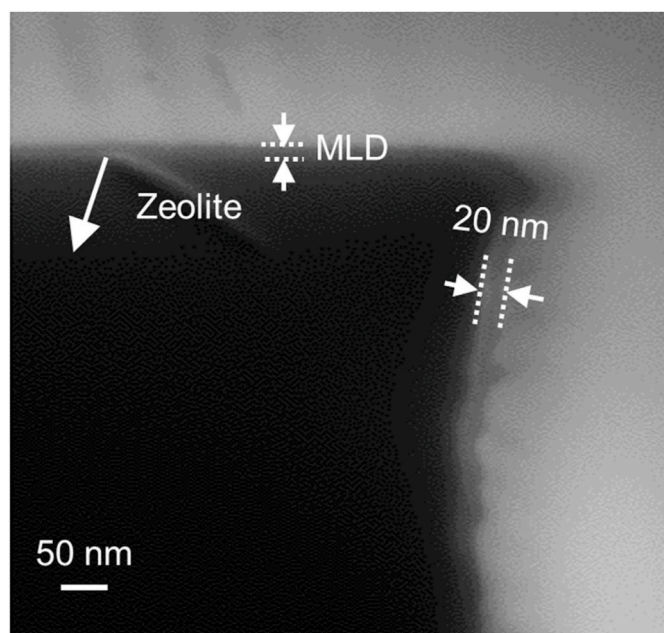


Fig. 2. FIB-SEM image of SSZ-13+30MLD membrane.

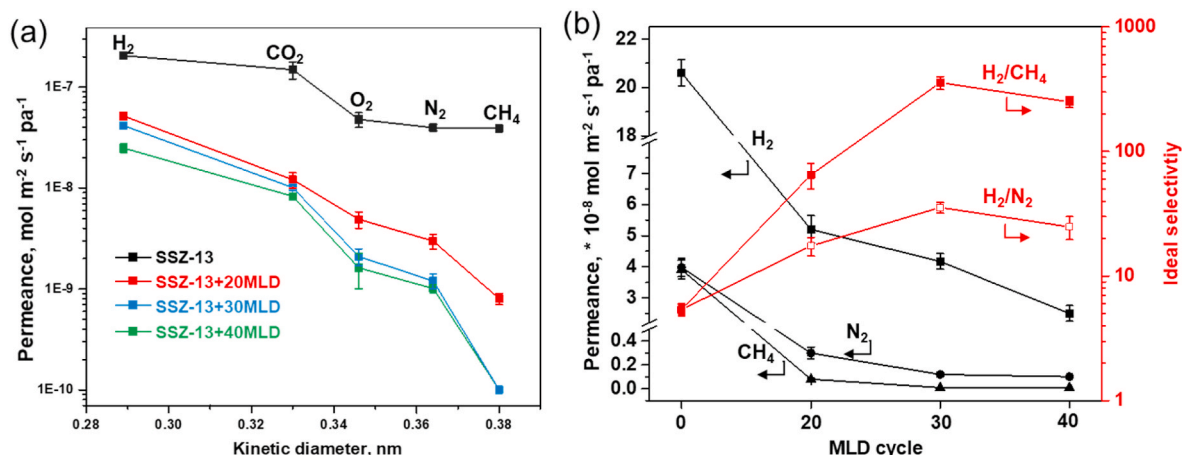


Fig. 3. (a) Gas permeance versus kinetic diameter for the pristine and MLD modified SSZ-13 membranes measured at 473 K and 10 bar transmembrane pressure drop. (b) H₂ permeance, H₂/N₂ and H₂/CH₄ ideal selectivity on different cycles MLD modified SSZ-13 membranes at 200 °C.

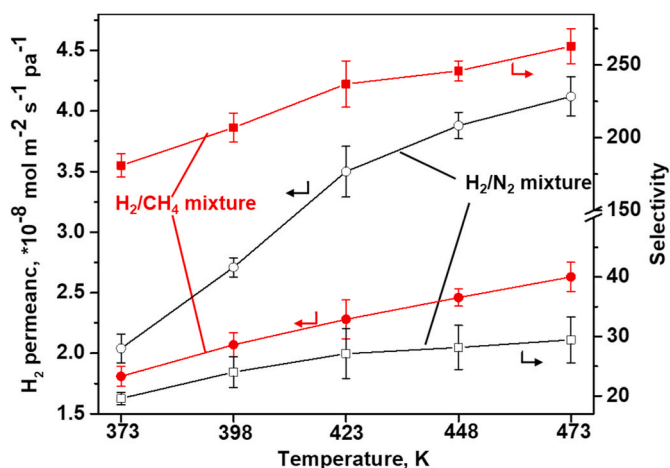


Fig. 4. Separation of 50%/50% H₂/N₂ mixture and 50%/50% H₂/CH₄ mixture by SSZ-13+30MLD at different temperatures. Transmembrane pressure drop is 2 bar with permeate pressure of 1 bar.

activated diffusion mechanism [27]. However, the increase of N₂ and CH₄ permeances were less than the increase of H₂ permeance with the increase of temperature. Therefore, both the H₂/N₂ and H₂/CH₄ selectivities increased from 19.9 to 28.4 and from 181 to 263, respectively, as the temperature increased from 373 K to 473 K. Equimolar H₂/CH₄ mixture separation through SSZ-13+30MLD membrane as a function of total pressure drop at 473 K was shown in Fig. S5. With the pressure drop increase from 2 to 10 bar, H₂ permeance gradually decreased while CH₄ permeance kept almost unchanged, thus resulting in decreased H₂/CH₄ selectivity. To demonstrate the stability of SSZ-13+30MLD membrane, long term H₂/CH₄ separation test was carried out at 10 bar for 48 h and the results (Fig. S6) confirmed the high stability of the MLD modified SSZ-13 membrane.

4. Conclusion

In summary, ultrathin microporous coatings were deposited on SSZ-13 membrane to eliminate the defects and reduce the zeolite pore mouth size. These MLD modified SSZ-13 membranes were more H₂ selective as compared with the pristine SSZ-13 membrane. The highest H₂/N₂ and H₂/CH₄ ideal selectivities of 35.6 and 427 were obtained on SSZ-13+30MLD. These MLD modified zeolite membranes are promising for H₂ separation in many fields, such as high-temperature hydroxylation

and dehydrogenation of organics and H₂ recovery in NH₃ synthesis, etc.

Associate content

FESEM of SSZ-13 membrane, XRD patterns of pristine and MLD modified SSZ-13 membranes, experimental apparatus for single and mixture gas permeation are described in the Supplementary materials.

CRediT authorship contribution statement

Qiaobei Dong: Data curation, Writing - original draft. **Ji Jiang:** Writing - original draft. **Shiguang Li:** Supervision, Funding acquisition. **Miao Yu:** Conceptualization, Supervision, Funding acquisition.

Declaration of competing interest

The authors declare that they have no known competing financial interests or personal relationships that could have appeared to influence the work reported in this paper.

Acknowledgment

We acknowledge the financial support from the Department of Energy (DOE) Advanced Research Projects Agency-Energy (ARPA-E) under Grant No. DE-AR0000931.

Appendix A. Supplementary data

Supplementary data to this article can be found online at <https://doi.org/10.1016/j.memsci.2020.119040>.

References

- [1] M. Momirlan, T. Veziroglu, Current status of hydrogen energy, *Renew. Sustain. Energy Rev.* 6 (2002) 141–179.
- [2] S. Sircar, T. Golden, Purification of hydrogen by pressure swing adsorption, *Separ. Sci. Technol.* 35 (2000) 667–687.
- [3] N.W. Ockwig, T.M. Nenoff, Membranes for hydrogen separation, *Chem. Rev.* 107 (2007) 4078–4110.
- [4] F. Zhou, H.N. Tien, Q. Dong, W.L. Xu, H. Li, S. Li, M. Yu, Ultrathin, ethylenediamine-functionalized graphene oxide membranes on hollow fibers for CO₂ capture, *J. Membr. Sci.* 573 (2019) 184–191.
- [5] F. Zhou, H.N. Tien, Q. Dong, W.L. Xu, B. Sengupta, S. Zha, J. Jiang, D. Behera, S. Li, M. Yu, Novel carbon-based separation membranes composed of integrated zero- and one-dimensional nanomaterials, *J. Mater. Chem. A* 8 (2020) 1084–1090.
- [6] H. Li, Z. Song, X. Zhang, Y. Huang, S. Li, Y. Mao, H.J. Ploehn, H.Y. Bao, M. Yu, Ultrathin, molecular-sieving graphene oxide membranes for selective hydrogen separation, *Science* 342 (2013) 95–98.

- [7] S.P. Cardoso, I.S. Azenha, Z. Lin, I. Portugal, A.E. Rodrigues, C.M. Silva, Inorganic membranes for hydrogen separation, *Separ. Purif. Rev.* 47 (2018) 229–266.
- [8] H. Li, K. Haas-Santo, U. Schygulla, R. Dittmeyer, Inorganic microporous membranes for H₂ and CO₂ separation-Review of experimental and modeling progress, *Chem. Eng. Sci.* 127 (2015) 401–417.
- [9] H. Wang, Y. Lin, Synthesis and modification of ZSM-5/silicalite bilayer membrane with improved hydrogen separation performance, *J. Membr. Sci.* 396 (2012) 128–137.
- [10] J. Choi, H.K. Jeong, M.A. Snyder, J.A. Stoeger, R.I. Masel, M. Tsapatsis, Grain boundary defect elimination in a zeolite membrane by rapid thermal processing, *Science* 325 (2009) 590–593.
- [11] H. Maghsoudi, Defects of zeolite membranes: characterization, modification and post-treatment techniques, *Separ. Purif. Rev.* 45 (2016) 169–192.
- [12] G. Xomeritakis, Z. Lai, M. Tsapatsis, Separation of xylene isomer vapors with oriented MFI membranes made by seeded growth, *Ind. Eng. Chem. Res.* 40 (2001) 544–552.
- [13] B. Zhang, C. Wang, L. Lang, R. Cui, X. Liu, Selective defect-patching of zeolite membranes using chemical liquid deposition at organic/aqueous interfaces, *Adv. Funct. Mater.* 18 (2008) 3434–3443.
- [14] J. Jiang, Q. Dong, F. Zhou, W.L. Xu, S. Li, M. Yu, Gel-modulated growth of high-quality zeolite membranes, *ACS Appl. Mater. Interfaces* 12 (2020) 26095–26100.
- [15] M. Hong, J.L. Falconer, R.D. Noble, Modification of zeolite membranes for H₂ separation by catalytic cracking of methyl-diethoxysilane, *Ind. Eng. Chem. Res.* 44 (2005) 4035–4041.
- [16] Z. Tang, J. Dong, T.M. Nenoff, Internal surface modification of MFI-type zeolite membranes for high selectivity and high flux for hydrogen, *Langmuir* 25 (2009) 4848–4852.
- [17] X. Liang, B.W. Evanko, A. Izar, D.M. King, Y.B. Jiang, A.W. Weimer, Ultrathin highly porous alumina films prepared by alucone ABC molecular layer deposition (MLD), *Microporous Mesoporous Mater.* 168 (2013) 178–182.
- [18] X. Liang, A.W. Weimer, An overview of highly porous oxide films with tunable thickness prepared by molecular layer deposition, *Curr. Opin. Solid State Mater. Sci.* 19 (2015) 115–125.
- [19] P. Sundberg, M. Karppinen, Organic and inorganic-organic thin film structures by molecular layer deposition: a review, *Beilstein J. Nanotechnol.* 5 (2014) 1104–1136.
- [20] Z. Song, Q. Dong, W.L. Xu, F. Zhou, X. Liang, M. Yu, Molecular layer deposition-modified 5A zeolite for highly efficient CO₂ capture, *ACS Appl. Mater. Interfaces* 10 (2017) 769–775.
- [21] Q. Dong, Z. Song, F. Zhou, H. Li, M. Yu, Ultrathin, fine-tuned microporous coating modified 5A zeolite for propane/propylene adsorptive separation, *Microporous Mesoporous Mater.* 281 (2019) 9–14.
- [22] S.I. Zones, Zeolite SSZ-13 and its method of preparation, US Patents US4544538A (1985).
- [23] Y. Huang, L. Wang, Z. Song, S. Li, M. Yu, Growth of high-quality, thickness-reduced zeolite membranes towards N₂/CH₄ separation using high-aspect-ratio seeds, *Angew. Chem. Int. Ed.* 54 (2015) 10843–10847.
- [24] Y. Zheng, N. Hu, H. Wang, N. Bu, F. Zhang, R. Zhou, Preparation of steam-stable high-silica CHA (SSZ-13) membranes for CO₂/CH₄ and C₂H₄/C₂H₆ separation, *J. Membr. Sci.* 475 (2015) 303–310.
- [25] Q. Dong, F. Zhou, J. Jiang, W. Xu, D.K. Behera, B. Sengupta, M. Yu, Advanced functional hierarchical nanoporous structures with tunable microporous coatings formed via an interfacial reaction processing, *ACS Appl. Mater. Interfaces* 12 (2020) 26360–26366.
- [26] P. Karakiliç, C. Huijskes, M.W. Luiten-Olieman, A. Nijmeijer, L. Winnubst, Sol-gel processed magnesium-doped silica membranes with improved H₂/CO₂ separation, *J. Membr. Sci.* 543 (2017) 195–201.
- [27] J.D. da Costa, G. Reed, K. Thambimuthu, High temperature gas separation membranes in coal gasification, *Energy Procedia* 1 (2009) 295–302.